Bioprocess Biosyst Eng (2011) 34:215–221
DOI 10.1007/s00449-010-0463-1

ORIGINAL PAPER

Hydrogen peroxide sensor based on Prussian blue electrodeposited on (3-mercaptopropyl)-trimethoxysilane polymer-modified gold electrode

Yu Zhang · Hong Qun Luo · Nian Bing Li

Received: 21 June 2010 / Accepted: 13 August 2010 / Published online: 27 August 2010

Abstract A hydrogen peroxide (H_2O_2) sensor was developed by electrodepositing Prussian blue (PB) on a gold electrode modified with (3-mercaptopropyl)-trimethoxysilane (MPS) polymer. The characterization of the self-assembled electrode was investigated by cyclic voltammetry and electrochemical impedance spectroscopy. The results of electrochemical experiments showed that such constructed sensor had a favorable catalytic ability to reduce H_2O_2. The MPS film on the modified gold electrode greatly enhanced the pH-adaptive range of PB. Large surface-to-volume ratio property of double-layer 2d-network MPS-modified PB electrode enabled stable and highly sensitive performance of the non-enzymatic H_2O_2 sensor. The linear range of H_2O_2 determined is from 2.0×10^{-6} to 2.0×10^{-4} mol L^{-1} with a correlation coefficient of 0.9991 and a detection limit for H_2O_2 of 1.8×10^{-6} mol L^{-1}. The influences of the potentially interfering substances on the determination of H_2O_2 were investigated. This modified electrode exhibits a good selectivity and high sensitivity with satisfactory results.

Keywords (3-Mercaptopropyl)-trimethoxysilane · Prussian blue · Hydrogen peroxide · Self-assembled monolayers

Introduction

In recent years, there has been a considerable interest in the reliable, accurate and rapid determination of hydrogen peroxide (H_2O_2) because it is an essential mediator in food, pharmaceutical, clinical, industrial and environmental analyses [1–3]. Hydrogen peroxide is also the by-product of many enzymatic reactions, so its concentration may be used as an indicator of the progress of a reaction [4–7]. Many techniques including titrimetry [8], spectrophotometry [9] and chemiluminescence [10] have been employed in the determination of H_2O_2. Recently, more attention has been paid to the electrochemistry technique because of its simplicity, intrinsic sensitivity and high selectivity [11, 12]. A large number of sensors based on the electrocatalysis of immobilized enzymes to H_2O_2 reduction were developed [13, 14]. For example, Dong's group [13] has developed a novel method to construct a third-generation horseradish peroxidase biosensor by self-assembling AuNPs into three-dimensional sol–gel network. The obtained electrochemical sensor exhibited good electrocatalytic performance toward H_2O_2. However, there still exist some practical problems related to the use of enzyme in these analytical devices, due to the short operational lifetimes and low reusability of these biocatalysts [15, 16]. Furthermore, the enzymes cannot obviously provide the biosensors a complete long-term stability due to their inherent instability [17]. Considering these aspects, it is necessary to develop a simple non-enzymatic sensor for determination of H_2O_2. Prussian blue (PB) could be an excellent substitute for peroxidase enzymes and mediator because of its particular catalytic activity.

Prussian blue is a prototype of metal hexacyanoferrates, which has well-known inherent electrochromic [18], photophysical [19], electrochemical [20] and molecular magnetic [21] properties. PB has been employed intensively as an electron transfer mediator for analytical applications and has been widely used in the biosensor development [22–25]. Due to its excellent electrocatalytic

Y. Zhang · H. Q. Luo · N. B. Li (✉)
Key Laboratory on Luminescence and Real-Time Analysis, Ministry of Education, School of Chemistry and Chemical Engineering, Southwest University, Chongqing 400715, People's Republic of China
e-mail: linb@swu.edu.cn

activity for the reduction of hydrogen peroxide, PB has been defined as an "artificial enzyme peroxidase", making it extremely attractive for constructing oxidoreductase-based biosensors [26–30].

Self-assembled monolayers (SAMs) technique has become a popular, simple and reliable procedure for voltammetric determination of organic and inorganic compounds, mostly because of its simplicity, versatility, well insulation and the establishment of a high level of order on a molecular scale as a means of preparing a modified surface [31]. The SAMs of chemisorption of thiols or disulfide on gold surfaces is of recent interest [32, 33]. It has been shown that organothiol molecules, upon adsorption on gold, lose hydrogen from the thiol group and an S–Au bond is then formed. The reaction mechanism between the S–H group and the Au atom is expressed as follows:

$$RSH + Au \rightarrow RS\text{-}Au + 1/2\,H_2$$

(3-Mercaptopropyl)-trimethoxysilane (MPS) is a bifunctional molecule that contains both thiol and silane functional groups; therefore, it was immobilized on the gold surface in virtue of the –SH of the MPS molecule serving as binding site for the covalent attachment of MPS. The hydrolyzed MPS monolayer was then used for the subsequent attachment of alkylsilanes [34]. In this paper, a detailed work was performed to investigate the preparation and properties of a hydrogen peroxide sensor based on the electrodeposition of PB on the self-assembled MPS. Prussian blue showed well-known excellent activity and selectivity toward the electrocatalytic reduction of H_2O_2. The electrochemical activities and determination of H_2O_2 were characterized by cyclic voltammogram and chronoamperometry. A fast and efficient quantitative method for the determination of H_2O_2 has been developed.

Experimental

Reagents

(3-Mercaptopropyl)-trimethoxysilane (MPS, 95%) was purchased from Aldrich. $K_3Fe(CN)_6$ and HCl were obtained from Chongqing Chuandong Chemical Reagent Plant, China. Hydrogen peroxide (30%), KCl and $FeCl_3$ were obtained from Chengdu Kelong Chemical Reagent Plant, China. All other chemicals were of analytical reagent grade and used as received. Phosphate buffer solutions (PBS) with various pH values were prepared with 0.1 M NaH_2PO_4 and 0.1 M Na_2HPO_4. Absolute ethanol was used as a solvent for MPS. The Piranha solution was prepared as described elsewhere (3:1 mixture of concentrated H_2SO_4 and 30% H_2O_2). Doubly distilled water was used throughout the experiments.

Apparatus

Electrochemical measurements were carried out on a CHI 660 (Shanghai Chenhua Instrument Co., China). The three-electrode system used in the measurements consisted of a gold electrode ($d = 2$ mm) as the working electrode, Pt as the counter electrode and an Ag/AgCl electrode as the reference electrode. All potentials were given with respect to the Ag/AgCl electrode. The pH S-3B meter (Shanghai Hongyi Instrumentation Co., LTD., China) was used to measure the pH.

Electrode preparation

The bare gold electrodes were mirror polished with 0.3 and 0.05 mm Al_2O_3 powder, respectively, and immersed in Piranha solution for 30 min, and then rinsed ultrasonically with water and absolute ethanol for 3 min. The electrodes were voltammetrically cycled in the potential range from 0 to 1.6 V in 0.1 mol L^{-1} H_2SO_4 solution until a stable cyclic voltammogram was obtained. The pretreated electrodes were immersed in 40 mmol L^{-1} MPS ethanol solution for 3 h at room temperature to produce a self-assembled monolayer and then washed thoroughly in ethanol. Subsequently, the electrodes were dipped into a 0.01 mol L^{-1} NaOH solution for 2 h to hydrolyze. Then the electrodes were soaked back into the MPS solution for 12 h. Thus, the membrane of MPS was formed on the gold electrodes (Au/MPS). To compare the electrochemical behaviors of different electrodes, two modified electrodes were prepared. One was prepared by electrodepositing PB on the bare gold electrode (Au/PB), and the other was prepared by electrodepositing PB on the MPS-modified gold electrode (Au/MPS/PB). The electrodeposition of PB was prepared by potential cycling at the scan rate of 50 mV s^{-1} in the potential range from −0.5 to +0.65 V (vs. Ag/AgC1) in a solution containing 2.5 mmol L^{-1} $FeCl_3$, 2.5 mmol L^{-1} $K_3Fe(CN)_6$, 0.1 mol L^{-1} KCl and 0.1 mol L^{-1} HCl. After deposition, the electrodes were thoroughly washed with doubly distilled water and then transferred into a supporting electrolyte solution (0.1 mol L^{-1} KCl + 0.1 mol L^{-1} HCl) and electrochemically activated by cycling between +350 and −50 mV (25 cycles) at a scan rate of 50 mV s^{-1}. Finally, the electrodes were rinsed with doubly distilled water again.

Electrochemical measurement

The electrochemical characteristics of the modified electrodes were characterized by cyclic voltammetry (CV) and electrochemical impedance spectroscopy (EIS) during the

fabrication process. Electrochemical experiments were performed in a conventional electrochemical cell containing a three-electrode system. CV experiment was performed at the potential swept from −0.2 to 0.6 V (vs. Ag/AgCl) at a scan rate of 100 mV s^{-1}. EIS experiment was performed in the frequency range from 0.1 to 10^5 Hz at the formal potential of 0.22 V. All experiments were conducted at room temperature.

Results and discussion

Cyclic voltammetry characterization of self-assembly process

Cyclic voltammetry is a simple and effective method for probing the feature of surface-modified electrode and testing the kinetic barrier of the interface, because the electron transfers between solution species and the electrode must be produced by tunneling either through the barrier or through the defects in the barrier. The CVs of the bare gold electrode and MPS-modified gold electrode in 5 mmol L^{-1} $K_3Fe(CN)_6$ solution containing 0.1 mol L^{-1} KCl are shown in Fig. 1. It is clearly shown that the $[Fe(CN)_6]^{4-/3-}$ redox couple can give a pair of well-defined reversible peaks at the bare gold electrode (Fig. 1a). When the layer of MPS was formed on the gold electrode, an obvious decrease in the cathodic and anodic peak currents can be observed (Fig. 1b). It might result from the blocking effect of the MPS on the electron transfer.

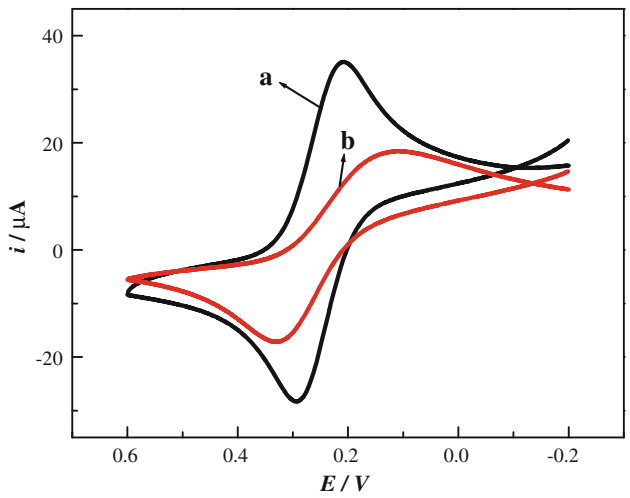

Fig. 1 Cyclic voltammograms of (**a**) the bare gold electrode, (**b**) the MPS-modified gold electrode in a solution containing 5 mmol L^{-1} $K_3Fe(CN)_6$ and 0.1 mol L^{-1} KCl. Scan rate, 100 mV s^{-1}

Electrochemical impedance spectroscopy characterization of self-assembly process

Electrochemical impedance spectroscopy (EIS) of $[Fe(CN)_6]^{4-/3-}$ solution is an effective and convenient method to give information on impedance change of the electrode surface in the modified process. Impedance measurements were performed in the frequency range from 0.1 to 10^5 Hz at the formal potential of 0.22 V in the 5 mmol L^{-1} $K_3Fe(CN)_6$ solution containing 0.1 mol L^{-1} KCl at the bare gold electrode and the MPS-modified gold electrode, respectively, and the results are shown in Fig. 2. The inset is the equivalent circuit, in which R_s is the solution resistance, C_{dl} is the double-layer capacitance, R_{et} is the electron transfer resistance and Z_w is the Warburg impedance. In EIS, the semicircle diameter of EIS equals the electron transfer resistance R_{et}. This resistance controls the electron transfer kinetics of redox probe ($[Fe(CN)_6]^{4-/3-}$) at the electrode interface. It can be seen from Fig. 2 that the bare gold electrode exhibited a very small semicircle domain, implying very low electron transfer resistance (R_{et} = 80.58 Ω, Fig. 2a) to the redox probe dissolved in the electrolyte solution. After the membrane of MPS was formed on the gold electrodes, the EIS of the resulting assembled MPS showed higher interfacial electron transfer resistance (R_{et} = 1,586 Ω, Fig. 2b), indicating the blocking effect of the MPS on the electron transfer. It is clear that the change of the impedance is consistent with that of cyclic voltammetry.

Characterization of PB film

Figure 3 shows the typical cyclic voltammograms (CVs) of the electrodeposition of PB on the MPS-modified gold

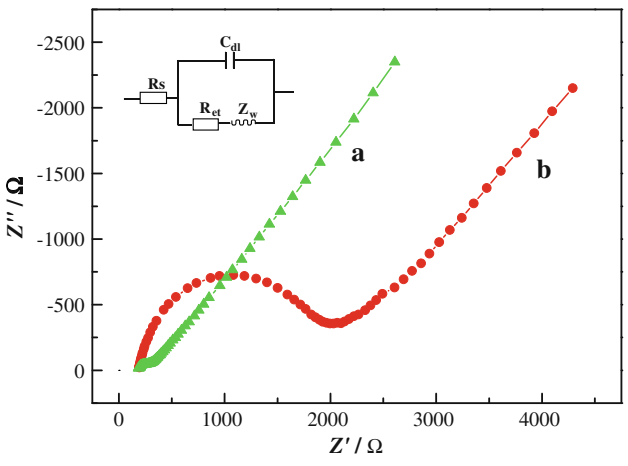

Fig. 2 Electrochemical impedance spectroscopy of 5 mmol L^{-1} $[Fe(CN)_6]^{3-}$ solution containing 0.1 mol L^{-1} KCl at the bare gold electrode (**a**) and the MPS-modified gold electrode (**b**). *Inset* shows the equivalent circuit model used to fit the impedance data

electrode in a solution containing 2.5 mmol L^{-1} $FeCl_3$, 2.5 mmol L^{-1} $K_3Fe(CN)_6$, 0.1 mol L^{-1} KCl and 0.1 mol L^{-1} HCl. It can be seen from Fig. 3 that a pair of redox peaks grow with the successive scans in the potential range of −0.5 to +0.65 V. The continuously increasing current indicates that PB is accumulating on the modified electrode.

Figure 4 displays a series of cyclic voltammograms (CVs) on the Au/MPS/PB-modified electrode obtained at different scan rates in 0.1 mol L^{-1} KCl solution containing 0.1 mol L^{-1} HCl as the supporting electrolyte and the dependence of the peak current on the square root of the scan rate. With the increase of the scan rate, the redox peak currents also increased gradually. The anodic and cathodic peak currents both increase linearly with the increase of the square root of the potential scan rate ($v^{1/2}$) between 20 and 140 mV s^{-1} (the inset of Fig. 4) with the correlation coefficients of −0.9929 and 0.9999, respectively, indicating that the electrode process is a diffusion-controlled process [35].

The dependence of peak current i_p on the scan rate v is described by the Randles–Sevcik equation:

$$i_p = \left(2.69 \times 10^5\right) n^{3/2} A D_0^{1/2} C_0 v^{1/2}$$

where n represents the number of electrons participating in the redox reaction, A is the area of the electrode (cm^2), D_0 is the diffusion coefficient of the molecules in the solution (cm^2 s^{-1}), C_0 is the concentration of the probe molecule in the bulk solution (mol cm^{-3}), v is the scan rate of the potential perturbation (V s^{-1}) and i_p is the peak current of the redox couple. In the equation, D_0, n and C_0 are constant

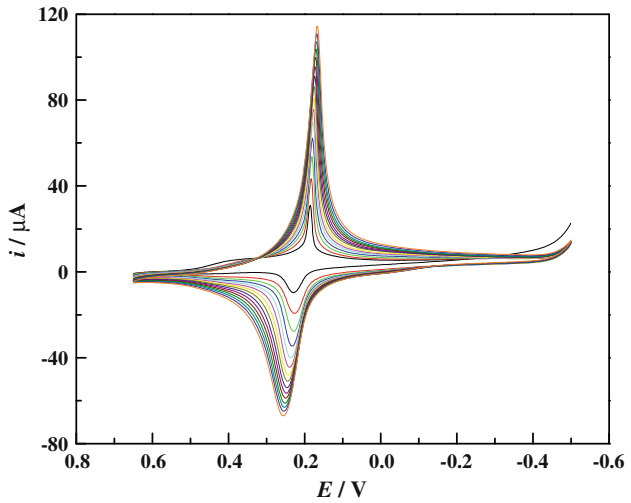

Fig. 3 Cyclic voltammograms of the MPS-modified gold electrode in a solution containing 2.5 mmol L^{-1} $FeCl_3$, 2.5 mmol L^{-1} $K_3Fe(CN)_6$, 0.1 mol L^{-1} KCl and 0.1 mol L^{-1} HCl in the potential range from −0.5 to +0.65 V at 50 mV s^{-1} for 15 cycles

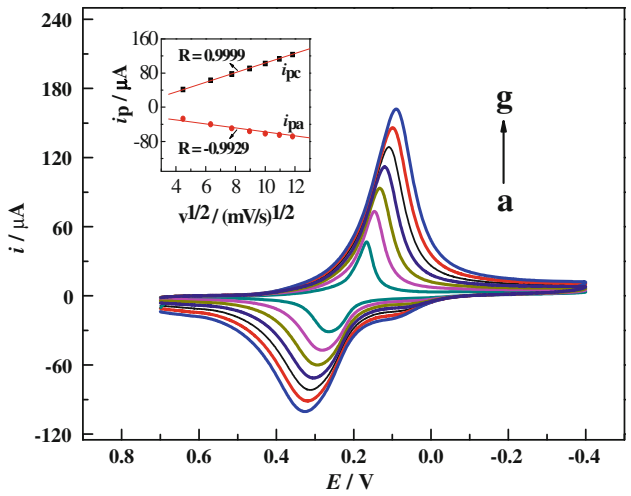

Fig. 4 Cyclic voltammograms of the Au/MPS/PB-modified electrode at different scan rates (from *a* to *g*): 20, 40, 60, 80, 100, 120 and 140 mV s^{-1} in 0.1 mol L^{-1} HCl solution containing 0.1 mol L^{-1} KCl under room temperature. The *inset* shows the dependence of redox peak currents on the square root of the scan rate

values, so the effective surface area (A) can be calculated from the value of $i_p/v^{1/2}$. The effective area of the modified electrode obtained by calculation was 0.235 cm^2, which is seven times larger than the area of the equivalent bare gold electrode (0.0314 cm^2).

Electrochemical characteristics of the modified electrodes

The effect of pH value on the electrochemical behavior of PB on the Au and Au/MPS electrodes in 0.1 mol L^{-1} PBS containing 0.1 mol L^{-1} KCl with different pH values has been investigated. For pH < 5.65, a pair of sharp redox peaks can be observed obviously on the Au/PB electrode. As the pH value increases to 7.0, the redox peak of PB begin to disappear. This implies that the electrochemical properties of PB at the Au electrode surface depend strongly on the pH value of the solution and the Au/PB electrode is not stable at near neutral solution. This phenomenon is probably ascribed to the strong interaction between ferric ions and hydroxyl ions (OH^-), which forms $Fe(OH)_3$ at higher pH, and it leads to the destruction of the Fe–CN–Fe bond and solubilization of PB [36]. However, for the Au/MPS/PB electrode, as the pH value increases to 8.50 and 9.77, both well-defined peaks can be observed obviously. As the pH value further increases to 10.46, the peaks are still observed. All these results indicate that the Au/MPS electrode greatly enhance the pH-adaptive range of PB, even to alkaline solution.

The surface coverages of PB on the Au/PB and Au/MPS/PB-modified electrodes in different pH value were

estimated from the cyclic voltammogram using the following equation [24]:

$$\Gamma = Q/nFA$$

where Q is the charge in coulombs, n is the number of electrons involved in the process, F is the Faraday constant, and A is the geometric area of the working electrode in square centimeters. The relationship between the surface coverage (Γ, using the cathodic peak located around 0.2 V) and pH for the Au/PB and Au/MPS/PB-modified electrodes are shown in Fig. 5. It can be illustrated from Fig. 5 that the surface coverage of PB on the Au/MPS-modified electrode is larger than that on the Au electrode. For the Au/MPS-modified electrode and Au electrode, the surface coverage of PB was almost unchanged when the pH value was lower than 6. It can be readily seen that the PB film on the Au electrode quickly loses stability at pH conditions above 6 (Fig. 5, curve a). However, the electroactivity of PB on the Au/MPS-modified electrode is almost the same as that in acidic solution, even when the pH reaches neutral condition (Fig. 5, curve b). After the pH is above 9.0, the PB electroactivity on the Au/MPS-modified electrode decreases rapidly. One of the reasons may be that the metal Fe of PB is strongly bonded with sulfur on the surface of the MPS network, so PB film can make a very strong combination on the electrode surface. Another reason is that PB can enter the cavity of the MPS network, and the network can resist the external pH changes in the environment. Thus, the network was expected to increase the stability of PB. All these results indicate that the Au/MPS/PB electrode greatly enhances the pH-adaptive range of PB and the stability of the modified electrode even in alkaline solution.

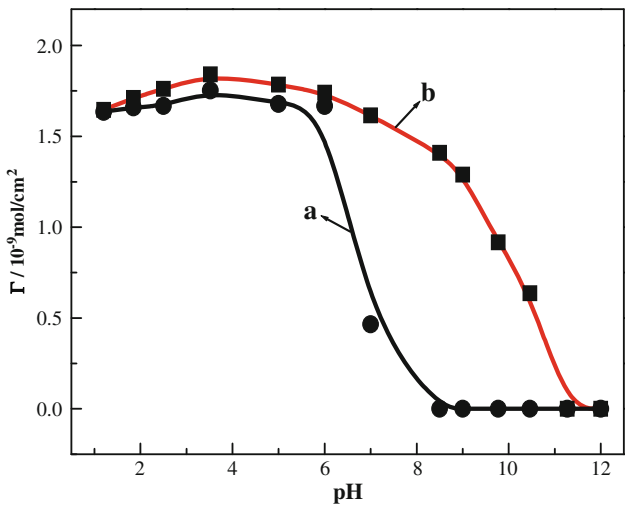

Fig. 5 Relationship between PB surface coverage (Γ) and pH of Au/PB (**a**) and Au/MPS/PB-modified electrodes (**b**)

Performance of the PB-modified electrode for H_2O_2 detection

The electrocatalytic activity for H_2O_2 (1.0 mol L^{-1}) on the Au/PB and Au/MPS/PB-modified electrodes were studied. The response of H_2O_2 on the Au/MPS/PB-modified electrode is higher than that on the Au/PB electrode, illustrating that the film of MPS enhances the electrocatalytic reduction of H_2O_2. Figure 6 shows a typical amperometric response of the Au/MPS/PB-modified electrode on successive injections of H_2O_2 into the stirring solution containing 0.1 mol L^{-1} HCl and 0.1 mol L^{-1} KCl at an applied potential of −0.2 V. The inset displays the relevant calibration curve for H_2O_2. When H_2O_2 was added into the stirring solution, the Au/MPS/PB-modified electrode responded rapidly. The linear range of H_2O_2 determined is from 2.0×10^{-6} to 2.0×10^{-4} mol L^{-1}. The regression equation is $i = 4.5617 + 0.04879\ C$(i, 10^{-6} A, C, μmol L^{-1}) with the correlation coefficient (r) of 0.9991 and the detection limit for H_2O_2 is 1.8×10^{-6} mol L^{-1}. The stability of the modified electrode and reproducibility of its electrocatalytic activity to H_2O_2 were examined. The stability of the Au/MPS/PB-modified electrode was studied by cyclic voltammetry in 0.1 mol L^{-1} KCl solution containing 0.1 mol L^{-1} HCl as the supporting electrolyte. Investigation indicated that the modified electrode exhibited a well-defined cyclic voltammogram with one pair of peaks at the potential range between +0.6 and −0.2 V (versus Ag/AgCl). After 200 continuous cycles at 100 mV s^{-1}, the peak heights of the cyclic voltammogram decreased <10%. The reproducibility of the sensor was also investigated. The relative standard deviation (RSD) was 4.5% for five replicated measurements at 10 μmol L^{-1} H_2O_2. Thus, the Au/MPS/PB-modified electrode was found to exhibit excellent stability and reproducibility.

Tolerance of potentially interfering substances

The influence of various potentially interfering species on the determination of 1.0×10^{-5} mol L^{-1} H_2O_2 was investigated and the results are shown in Fig. 7. The tolerance limit was taken as the maximum concentration of the potentially interfering substances, which caused an approximately ±5% relative error in the determination. The tolerated ratio of the potentially interfering substances was 40 for glycine acid, 20 for glucose and glutamic acid, 5 for citric acid, and 1 for uric acid, ascorbic acid and nitrite.

Analytical application

The sample analysis of H_2O_2 was studied in tap water sample, which was collected from our laboratory. Into a 10 mL calibrated flask, 3.0 mL of the water sample was

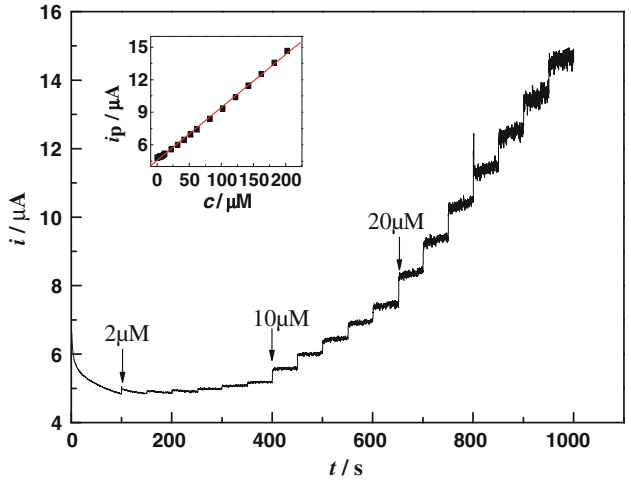

Fig. 6 Typical steady-state response of the sensor to successive injection of H_2O_2 into the stirring solution containing 0.1 mol L^{-1} HCl and 0.1 mol L^{-1} KCl. The *inset* displays the calibration curve for H_2O_2. Applied potential: −0.2 V

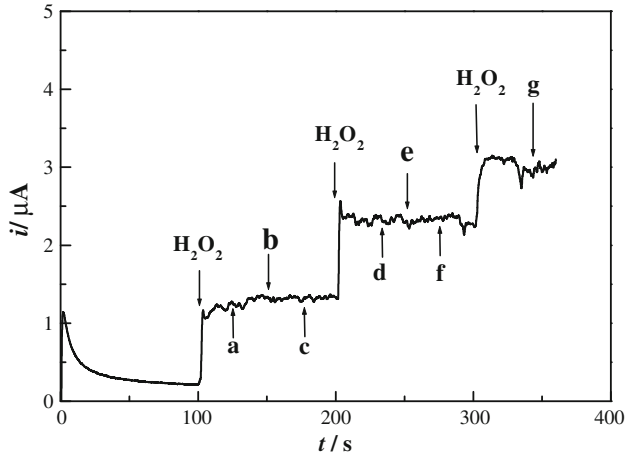

Fig. 7 Current-time curve recorded at the sensor for addition of (*a*) 1.0×10^{-5} mol L^{-1} ascorbic acid, (*b*) 1.0×10^{-5} mol L^{-1} uric acid, (*c*) 2.0×10^{-4} mol L^{-1} glucose, (*d*) 2.0×10^{-4} mol L^{-1} glutamic acid, (*e*) 4.0×10^{-4} mol L^{-1} glycine acid, (*f*) 5.0×10^{-5} mol L^{-1} citric acid and (*g*) 1.0×10^{-5} mol L^{-1} nitrite into the stirring solution containing 0.1 mol L^{-1} HCl and 0.1 mol L^{-1} KCl, respectively. Applied potential: −0.2 V

pipetted and H_2O_2 determined. H_2O_2 was not found in the tap water. So the recovery test was carried out by adding different amounts of H_2O_2 standards in the sample matrix, and the experimental results are shown in Table 1.

Conclusions

In this paper, we have prepared a hydrogen peroxide sensor based on the self-assembled MPS and the electrodeposition of PB. Prussian blue showed electrocatalytic activity for the reduction of H_2O_2. The resulted sensor exhibited much wider pH-adaptive range, extremely fast amperometric response, a low detection limit and a wide linear range to H_2O_2. Besides, the modified electrode exhibits good selectivity and sensitivity.

Table 1 Recovery for the determination of H_2O_2 in the tap water sample

Sample	Original (μmol L^{-1})	Added (μmol L^{-1})	Found[a] (μmol L^{-1})	RSD (%)	Recovery (%)
Tap water	ND	10.00	9.81	1.03	98.10
	ND	30.00	29.03	1.55	96.77
	ND	50.00	48.50	2.73	97.00

ND not detected

[a] Mean of three determinations

Acknowledgments This project was supported by the National Natural Science Foundation of China (No. 20575054), China (NSFC)-Korea (KOSEF) Joint Research Project (No. 20811140329) and the Municipal Science Foundation of Chongqing City (No. CSTC-2008BB4012, CSTC-2008BB4013), and all authors here express their deep thanks.

References

1. Bartlett PN, Birkin PR, Wang JH, Palmisano F, Benedetto GD (1998) An enzyme switch employing direct electrochemical communication between horseradish peroxidase and a poly(aniline) film. Anal Chem 70:3685–3694
2. Sellers RM (1980) Spectrophotometric determination of hydrogen peroxide using potassium titanium(IV) oxalate. Analyst 105:950–954
3. Wolfbeis O, Drkop A, Wu M, Lin Z (2002) A europium-ion-based luminescent sensing probe for hydrogen peroxide. Angew Chem Int Ed 41:4495–4498
4. Salimi A, Miranzadeh L, Hallaj R, Mamkhezri H (2008) Picomolar detection of hydrogen peroxide at glassy carbon electrode modified with NAD^+ and single walled carbon nanotubes. Electroanal 20:1760–1768
5. Darder M, Takada K, Pariente F, Lorenzo E, Abruna HD (1999) Dithiobissuccinimidyl propionate as an anchor for assembling peroxidases at electrodes surfaces and its application in a H_2O_2 biosensor. Anal Chem 71:5530–5537
6. Masullo M, Raimo G, Russo AD, Bocchini V, Bannister JV (1996) Purification and characterization of NADH oxidase from the Archaea *Sulfolobus acidocaldarius* and *Sulfolobus solfataricus*. Biotechnol Appl Biochem 23:47–54
7. Bhate RH, Ramasarma T (2010) Catalase-dependent release of half of the consumed oxygen during the activity of potato mitochondrial alternative oxidase confirms H_2O_2 as the product of oxygen reduction. Arch Biochem Biophys 495:95–96
8. Hurdis EC, Romeyn H (1954) Accuracy of determination of hydrogen peroxide by cerate oxidimetry. Anal Chem 26:320–325
9. Luo W, Abbas ME, Zhu LH, Deng KJ, Tang HQ (2008) Rapid quantitative determination of hydrogen peroxide by oxidation decolorization of methyl orange using a Fenton reaction system. Anal Chim Acta 629:1–5

10. Chen WW, Li BX, Xu CL, Wang L (2009) Chemiluminescence flow biosensor for hydrogen peroxide using DNAzyme immobilized on eggshell membrane as a thermally stable biocatalyst. Biosens Bioelectron 24:2534–2540
11. Sheng QL, Yu H, Zheng JB (2007) Hydrogen peroxide determination by carbon ceramic electrodes modified with pyrocatechol violet. Electrochim Acta 52:7300–7306
12. Luo XL, Xu JJ, Zhang Q, Yang GJ, Chen HY (2005) Electrochemically deposited chitosan hydrogel for horseradish peroxidase immobilization through gold nanoparticles self-assembly. Biosens Bioelectron 21:190–196
13. Jia JB, Wang BQ, Wu AG, Cheng GJ, Li Z, Dong SJ (2002) A method to construct a third-generation horseradish peroxidase biosensor: self-assembling gold nanoparticles to three-dimensional sol–gel network. Anal Chem 74:2217–2223
14. Guo SJ, Wang EK (2007) Synthesis and electrochemical applications of gold nanoparticles. Anal Chim Acta 598:181–192
15. Gavalas VG, Chaniotakis NA (2001) Phosphate biosensor based on polyelectrolyte-stabilized pyruvate oxidase. Anal Chim Acta 427:271–277
16. Gavalas VG, Chaniotakis NA (2000) Polyelectrolyte stabilized oxidase based biosensors: effect of diethylaminoethyl-dextran on the stabilization of glucose and lactate oxidases into porous conductive carbon. Anal Chim Acta 404:67–73
17. Zou GZ, Ju HX (2004) Electrogenerated chemiluminescence from a CdSe nanocrystal film and its sensing application in aqueous solution. Anal Chem 76:6871–6876
18. Kulesza PJ, Miecznikowski K, Chojak M, Malik MA, Zamponi S, Marassi R (2001) Electrochromic features of hybrid films composed of polyaniline and metal hexacyanoferrate. Electrochim Acta 46:4371–4378
19. Pyrasch M, Tieke B (2001) Electro- and photoresponsive films of Prussian blue prepared upon multiple sequential adsorption. Langmuir 17:7706–7709
20. Marco O, Pamela A, Rodrigo DR, Ricardo S, Ricardo C, Fritz S, Heike K (2005) Chronocoulometric study of the electrochemistry of Prussian blue. J Phys Chem B 109:15483–15488
21. Zhou P, Xue D, Luo H, Chen X (2002) Fabrication, structure, and magnetic properties of highly ordered Prussian blue nanowire arrays. Nano Lett 2:845–847
22. Karyakin AA, Karyakin EE (1999) Prussian blue-based 'artificial peroxidase' as a transducer for hydrogen peroxide detection. Application to biosensors. Sens Actuators B 57:268–273
23. Karyakin AA, Karyakina EE, Gorton L (2000) Amperometric biosensor for glutamate using Prussian blue-based "artificial peroxidase" as a transducer for hydrogen peroxide. Anal Chem 72:1720–1723
24. Li NB, Park JH, Park K, Kwon SJ, Shin H, Kwak J (2008) Characterization and electrocatalytic properties of Prussian blue electrochemically deposited on nano-Au/PAMAM dendrimer-modified gold electrode. Biosens Bioelectron 23:1519–1526
25. Liu Y, Chu ZY, Jin WQ (2009) A sensitivity-controlled hydrogen peroxide sensor based on self-assembled Prussian blue modified electrode. Electrochem Commun 11:484–487
26. Razmi H, Mohammad-Rezaei R, Heidari H (2009) Self-assembled Prussian blue nanoparticles based electrochemical sensor for high sensitive determination of H_2O_2 in acidic media. Electroanalysis 21:2355–2362
27. Li YH, Liu XY, Zeng XD, Liu Y, Liu XS, Wei WZ, Luo SL (2009) Nonenzymatic hydrogen peroxide sensor based on a Prussian blue-modified carbon ionic liquid electrode. Microchim Acta 165:393–398
28. Zou YJ, Sun LX, Xu F (2007) Biosensor based on polyaniline–Prussian blue/multi-walled carbon nanotubes hybrid composites. Biosens Bioelectron 22:2669–2674
29. Li ZF, Chen JH, Li W, Chen K, Nie LH, Yao SZ (2007) Improved electrochemical properties of Prussian blue by multi-walled carbon nanotubes. J Electroanal Chem 603:59–66
30. Tseng KS, Chen LC, Ho KC (2005) Amperometric detection of hydrogen peroxide at a Prussian blue-modified FTO electrode. Sens Actuators B 108:738–745
31. Zhou YM, Wu ZY, Shen GL, Yu RQ (2003) An amperometric immunosensor based in Nafion-modified electrode for determination of *Schistosoma japonicum* antibody. Sens Actuators B 89:292–298
32. Ritzert NL, Casella SS, Zapien DC (2009) Surface-electrochemistry of ferritin adsorbed on 8-mercaptooctanoic acid-modified gold electrodes. Electrochem Commun 11:827–830
33. Wu Y, Li NB, Luo HQ (2008) Electrochemical determination of Pb(II) at a gold electrode modified with a self-assembled monolayer of 2, 5-dimercapto-1, 3, 4-thiadiazole. Microchim Acta 160:185–190
34. Cai M, Ho M, Pemberton JE (2000) Surface vibrational spectroscopy of alkylsilane layers covalently bonded to monolayers of (3-mercaptopropyl)-trimethoxysilane on Ag substrates. Langmuir 16:3446–3453
35. Yu L, Zhang G, Wu Y, Bai X, Guo D (2008) Cupric oxide nanoflowers synthesized with a simple solution route and their field emission. J Cryst Growth 310:3125–3130
36. Karyakin AA, Karyakin EE, Gorton L (1999) On the mechanism of H_2O_2 reduction at Prussian blue modified electrodes. Electrochem Commun 1:78–82